

# Vertical urban growth monitoring through PSInSAR Stack On-Off model approach: A case study of Wuhan (2015–2024)

Zeeshan Afzal, Timo Balz, Sunantha Ousaha, Cem Sönmez Boyoğlu

State Key Laboratory of Information Engineering in Surveying, Mapping and Remote Sensing, Wuhan University, Wuhan 430079, China

2018276190014@whu.edu.cn , balz@whu.edu.cn , sunantha.sun@hotmail.com , cemonmezboyoglu@gmail.com

**Keywords:** Vertical urban growth, PSInSAR Stack On-Off model, Sentinel-1, building height estimation, Wuhan

## Abstract

Monitoring vertical urban growth is crucial for understanding urban development patterns and supporting informed city planning decisions. This study introduces a novel PSInSAR Stack On-Off model approach for efficient monitoring of vertical urban growth, applied to Wuhan, China, using Sentinel-1 data from 2015 to 2024. The methodology streamlines traditional PSInSAR processing by initially focusing on recent imagery for PS point extraction before analyzing the complete temporal stack, significantly reducing computational requirements while maintaining monitoring capabilities. Analysis of the spatial-temporal patterns shows distinct development phases, with 64.81% of structures predating 2015, followed by more targeted development in subsequent periods. The results show significant variations in vertical growth across districts, with Jiangnan emerging as the most vertically developed area (mean height 29.4m) and clear correlation between building heights and proximity to the Yangtze River. Three distinct district typologies were identified: High-Intensity Vertical, Mixed-Development, and Horizontal Expansion, reflecting differentiated urban development strategies. This study demonstrates the effectiveness of the Stack On-Off approach for monitoring urban vertical growth, providing valuable insights for urban planning and development in rapidly growing metropolitan areas.

## 1. Introduction

Urbanization is a defining global trend, with over half of the world's population currently residing in urban areas, and this proportion is projected to reach 68% by 2050 (United Nations, 2018). This rapid and often unplanned urban growth poses significant challenges for urban planning, resource management, and environmental sustainability (UN Desa, 2019). Monitoring urban expansion is crucial for informed decision-making, but traditional methods often struggle to capture the full complexity of urban dynamics, particularly in the vertical dimension.

While horizontal urban expansion, often referred to as urban sprawl, is relatively well-studied using remote sensing techniques like multispectral imagery analysis and nighttime light data (Zhang and Seto, 2011; Li et al., 2020a), vertical growth presents greater challenges. Traditional remote sensing methods, primarily focused on two-dimensional changes, often fail to adequately capture the construction of taller buildings and the intensification of land use through multi-story developments. Techniques like LiDAR and photogrammetry can provide accurate height information, but they are often costly and limited in temporal coverage, making them unsuitable for frequent, large-scale monitoring (Li et al., 2020b; Liu et al., 2020).

Persistent Scatterer Interferometric Synthetic Aperture Radar (PSInSAR), a specialized variant of SAR Interferometry (InSAR), has emerged as a powerful technique for measuring surface deformation and structural changes with millimeter-level precision (Afzal et al., 2023; Ferretti et al., 2001). This technique identifies stable, highly reflective points—known as persistent scatterers—that maintain Amplitude Stability over extended time periods, enabling precise monitoring of subtle movements in urban environments.

While PSInSAR was originally developed for deformation monitoring, researchers have successfully adapted it for various urban applications, including the detection of new construction and vertical urban growth (VUG) (Letsios et al., 2023; Prakash

et al., 2023). However, applying PSInSAR to VUG analysis presents several significant challenges. First, building height estimation is complicated by the fact that persistent scatterers can be located anywhere on a building's surface, making it difficult to determine the actual building height. Additionally, traditional PSInSAR processing must be modified to detect building construction, typically through the implementation of an On-off model. This conventional approach, which requires processing the entire dataset to estimate the Amplitude Stability Index (ASI), can be computationally intensive—for example, in our experimental testing, processing 212 Sentinel-1 images of Wuhan using the traditional PSInSAR on-off method required approximately a week processing time on a standard workstation (Intel Core i5, 16GB RAM).

To address these limitations, this study introduces a PSInSAR stack "On/Off" methodology for monitoring vertical urban growth in Wuhan, China, using Sentinel-1 data. The proposed approach efficiently detects both building construction and heights by utilizing the amplitude stability characteristics of persistent scatterers. This refinement significantly reduces computational requirements while maintaining monitoring capability, making it particularly suitable for long-term, large-scale detection of vertical urban expansion. Beyond advancing PSInSAR methodology, this research provides critical insights into urban vertical growth patterns in rapidly developing metropolitan areas.

## 2. Study area

Wuhan (30°35'N, 114°17'E), the capital of Hubei Province, China, is a rapidly growing megacity strategically located at the confluence of the Yangtze and Han Rivers. It serves as a major economic, political, cultural, and educational center in Central China (Sun et al., 2023). The city covers a total administrative area of 8,494.41 square kilometers, of which the urban built-up

area comprises approximately 1,528 square kilometers (Wuhan Municipal Statistics Bureau, 2020).

The city is divided into three major districts by the rivers: Wuchang, Hankou, and Hanyang, historically known as the "Three Towns of Wuhan." These districts, along with ten other administrative districts (Dongxihu, Caidian, Hanyang, Qiaokou, Jiangxia, Hongshan, Jiangnan, Jiang'an, and Qingshan), form the contemporary metropolitan area (Wang et al., 2018).

Wuhan has experienced accelerated urbanization over the past two decades, epitomizing the rapid urban transformation seen across many Chinese cities. The city's population surged from approximately 8 million in 2000 to over 12 million in 2020, reflecting an average annual growth rate of 2.1% (Wuhan Municipal Statistics Bureau, 2020; China Statistics Press, 2020; Wang et al., 2022). This growth has been accompanied by significant vertical expansion, making Wuhan a prime example of the shift from horizontal to vertical development in response to land scarcity and population pressure. The city's skyline has been dramatically reshaped, with the number of buildings exceeding 100 meters in height and now considered as the 8th tallest city in the world

(<https://www.skyscrapercenter.com/city/wuhan>).

### 3. Dataset and Methodology

This study employs Synthetic Aperture Radar (SAR) data exclusively from the Sentinel-1A satellite, part of the European Space Agency's (ESA) Copernicus Programme. Sentinel-1A was launched on April 3, 2014, and operates in a near-polar, sun-synchronous orbit at an altitude of 693 km with a 12-day repeat cycle (Torres et al., 2012). The dataset consists of Single Look Complex (SLC) products acquired by Sentinel-1A in Interferometric Wide (IW) swath mode, which employs the Terrain Observation with Progressive Scans (TOPS) technique (Yague-Martinez et al., 2016). The IW mode provides a nominal spatial resolution of 5 m in range and 20 m in azimuth, with a swath width of 250 km. The acquisition mode operates with incidence angles ranging from 29.1° to 46.0° and utilizes VV (Vertical-Vertical) polarization with a 12-day repeat cycle. VV polarization was selected based on its demonstrated effectiveness in urban monitoring applications, particularly its sensitivity to vertical structures through double-bounce scattering mechanisms characteristic of building facades (Crosetto et al., 2016).

The core of our methodology is a novel PSInSAR stack "On/Off" approach, illustrated in Figure 1. This approach streamlines the traditional PSInSAR workflow by focusing on a subset of recent images (March 2023 - April 2024) for initial PS point extraction and then extraction of date of construction of the buildings from the whole dataset from 2015 to 2024



Figure 1. Workflow of the PSInSAR-based vertical urban growth monitoring methodology.

The key steps of the methodology are detailed below:

**3.1 Data Preparation:** A master image was carefully selected from June 15, 2020, based on criteria that minimized both temporal and spatial decorrelation. This optimization is crucial for ensuring the accuracy of the interferometric measurements. Image coregistration, a critical step to align all images to the master, was performed using the Enhanced Spectral Diversity (ESD) method, achieving sub-pixel accuracy of better than 0.001 pixels in azimuth (Yague-Martinez et al., 2016). This high level of accuracy is essential for detecting subtle changes in building heights.

### 3.2 PS Point Extraction (Recent Imagery):

Persistent Scatterer (PS) points were extracted from the 30 most recent images (March 2023 - April 2024). This was accomplished by calculating the Amplitude Stability Index (ASI), defined as (Ferretti et al., 2001):

$$ASI = 1 - \frac{\sigma_{amp}}{\mu_{amp}} \quad (1)$$

where  $\sigma_{amp}$  is the temporal standard deviation of amplitude; and  $\mu_{amp}$  denotes the mean amplitude across the temporal series.

The extracted PS points, initially in radar geometry, were geocoded to geographic coordinates (latitude and longitude) using the SAR image metadata and orbit information. This step is essential for linking the PS points with real-world locations.

A sophisticated dual-threshold strategy was implemented:

- Higher threshold (0.80) for points used in atmospheric phase screen estimation
- Lower threshold (0.7) for PS point selection in Multi image sparse point processing.

PS points represent stable reflectors on the Earth's surface, such as buildings or infrastructure, that exhibit minimal amplitude variability over time. This focused approach, using only recent imagery enable us to avoid the need to process the entire time series for initial PS selection, thereby significantly reducing computational time and resources compared to PSInSAR On-off technique.

### 3.3 APS Estimation:

Atmospheric Phase Screen (APS) estimation was then applied using Delaunay triangulation to connect the PS points into a network of triangles. This network served as the basis for estimating and removing atmospheric phase delays, which can introduce significant errors in height and displacement calculations. Height and velocity estimation parameters of 200 m and 100 mm/year, respectively, were used. These parameters were chosen based on prior knowledge of typical building heights and urban growth trends in Wuhan, as well as the characteristics of the Sentinel-1 data.

### 3.4 Reference Point Selection:

A stable reference point is crucial for accurate PSInSAR analysis. After testing several potential reference points, a point with latitude 30.44°N and longitude 114.25°E was selected as the most stable. This point exhibited minimal height differences compared to surrounding buildings and a consistently high ASI value throughout the entire time series.

The relative height measurement ( $\Delta h$ ) between any PS point and the reference point is calculated using:

$$\Delta h = \frac{\lambda R \sin \theta}{4\pi B_{\perp}} \phi_{int} \quad (2)$$

where  $\Delta h$  is the height difference relative to the reference point;  $B_{\perp}$  is the perpendicular baseline;  $R$  is the slant range distance;  $\theta$  is the incidence angle;  $\lambda$  is the radar wavelength.

However, this equation assumes an unwrapped interferometric phase ( $\phi_{int}$ ), while in reality, the measured phase is wrapped within the interval  $[-\pi, \pi]$ . This phase wrapping introduces ambiguity in height estimation, as multiple possible height values could correspond to the same wrapped phase measurement. This limitation makes it challenging to accurately determine building heights solely from the interferometric phase. Therefore, our methodology incorporates amplitude stability analysis (detailed in sections 3.5 and 3.6) to complement and strengthen the height estimation process

This reference point served as the baseline for all subsequent height and displacement calculations, with the relative heights of all other PS points calculated with respect to this reference.

### 3.5 Sparse Point Processing:

To refine the PS point selection, we empirically determined an optimal ASI threshold of 0.7 through iterative testing of different threshold values (0.65, 0.70, 0.75, and 0.80). This threshold value was selected based on two key criteria: point stability and spatial distribution quality. While higher thresholds ( $>0.75$ ) yielded more stable points, they significantly reduced the total number of PS points, particularly in urban areas. Conversely, lower thresholds ( $<0.7$ ) introduced noise, especially along the riverside where PS points are theoretically impossible due to water's unstable reflection characteristics. The chosen threshold of 0.7 optimizes this trade-off, ensuring sufficient point stability for reliable height and velocity estimation while maintaining comprehensive spatial coverage of the urban area. This balanced approach enables robust analysis of vertical urban development patterns while minimizing false positives in non-building areas. To assess the reliability and accuracy of height measurements, we calculate two key quality metrics. First, the temporal coherence ( $\gamma$ ) provides a measure of phase stability over time:

$$\gamma = \frac{|\sum_{i=1}^N e^{j(\phi_{i,obs} - \phi_{i,mod})}|}{N} \quad (3)$$

where  $\phi_{i,obs}$  and  $\phi_{i,mod}$  represent the observed and modeled interferometric phases respectively, and  $N$  is the number of interferograms.

To quantify the uncertainty in height measurements, we estimate the residual height error variance as (Perissin, 2017):

$$\sigma_{\Delta h}^2 = \left(\frac{\lambda R \sin \theta}{4\pi}\right)^2 \frac{\sigma_{\Delta \phi}^2}{N \sigma_{B_{\perp}}^2} \quad (4)$$

where  $\Delta h$  is the height,  $\Delta \phi$  is the observation phase,  $B_{\perp}$  is the normal baseline and  $\lambda$ ,  $\theta$ ,  $R$  are the sensor wavelength, incidence angle, and sensor-to-target distance, respectively. These metrics together provide a comprehensive assessment of measurement quality and enable us to identify and filter unreliable height estimates.

### 3.6 Amplitude Time Series Analysis (Full Stack):

The ASI was recalculated for all 228 images (2015-2024) only for the selected PS points that passed the ASI threshold in the previous step. For each point  $p$  at time  $t$ , the ASI is calculated using a forward-looking temporal window:

$$ASI(p, t) = 1 - \frac{\sigma_{amp}(t, t_{end})}{\mu_{amp}(t, t_{end})} \quad (5)$$

where  $\sigma_{amp}(t, t_{end})$  is the standard deviation of amplitude from time  $t$  to the end of the series;  $\mu_{amp}(t, t_{end})$  is the mean amplitude from time  $t$  to the end of the series. The "On/Off" concept is applied to detect construction and demolition events:

$T_{ON}$  (Birth): A PS point is classified as "born," indicating the construction or completion of a building, when its ASI rises above the 0.7 threshold and remains consistently stable above this value in subsequent images. Mathematically:

$$T_{ON} = \min\{t \in T | ASI(p, t) > 0.7\} \quad (6)$$

$T_{OFF}$  (Death): A PS point is classified as "dead," indicating the demolition or structural degradation of a building, when its ASI falls below the 0.7 threshold and continues to decline in subsequent images.

$$T_{OFF} = \min\{t \in T | t > T_{ON} \wedge ASI(p, t) < 0.7\} \quad (7)$$

This step-wise ASI calculation approach provides a robust method for detecting the emergence and potential disappearance of persistent scatterers throughout the time series, enabling accurate tracking of structural changes in the urban environment.

### 3.7 Geospatial Mapping and Analysis:

The derived  $T_{ON}$  and  $T_{OFF}$  dates, combined with the estimated height information for each PS point, were used to generate maps and time series of vertical urban growth. The spatial analysis framework incorporates density-based spatial clustering (DBSCAN) to identify coherent groupings of persistent scatterers. The DBSCAN algorithm defines neighborhoods of points according to:

$$N_{\epsilon}(p) = \{q \in D | dist(p, q) \leq \epsilon\} \quad (8)$$

where  $N_{\epsilon}(p)$  represents the neighborhood of point  $p$  within the dataset  $D$ ;  $\epsilon$  is the radius parameter set to 0.03 in this implementation;  $dist(p, q)$  is a distance function that measures the spatial proximity between points  $p$  and  $q$ .

Dynamic grids were employed to calculate the average height growth within different districts of Wuhan. Statistical filtering within each grid cell employs the Interquartile Range (IQR) method to identify and remove potential outliers:

$$IQR = Q_3 - Q_1 \quad (9)$$

$$Outliers = \{x : x < Q_1 - 1.5 \times IQR \text{ or } x > Q_3 + 1.5 \times IQR\} \quad (10)$$

where  $Q_1$  and  $Q_3$  represent the first and third quartiles of height values within each cell.

Each grid contained multiple PS points, and the maximum height within each grid was extracted to represent the overall height of buildings in that region. This provided a spatial and temporal analysis of the city's evolving skyline, allowing for the identification of areas with rapid vertical expansion.

## 4. Results

The PSInSAR "On/Off" analysis of Sentinel-1 data revealed significant, spatially varied, and temporally dynamic vertical urban growth in Wuhan between 2015 and 2023. The method

efficiently quantified not just the extent of height changes but also the patterns of development across the city.

#### 4.1 PS Height and Temporal Relationships

Figure 2 presents a detailed analysis of temporal patterns through three complementary visualizations. The annual new PS distribution graph (top left) shows that by 2015, Wuhan had accumulated approximately 350,000 PS points throughout its development. After 2015, new PS detections stabilized at around 25,000-30,000 points annually from 2018 onwards, reflecting contemporary urban development patterns.

The PS height distribution histogram (top right) demonstrates that most scatterers are detected within the 0-25m range, with significantly fewer points detected above 50m in height. The distribution exhibits a dominant peak around 10m, with a secondary concentration near 25m, suggesting typical height ranges where stable scatterers are most commonly found in the urban environment.

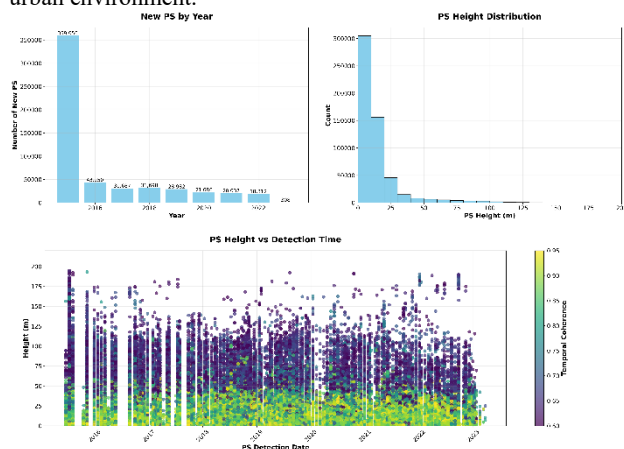


**Figure 2.** Temporal Analysis of New PS, PS Height Distribution, and Temporal Coherence in Wuhan (2015–2023). (Top Left) New PS per year. (Top Right) PS height distribution. (Bottom) Coherence vs. PS height.

##### 4.1.1 Temporal Coherence Analysis and Height Reliability

The bottom panel of Figure 2 presents a crucial relationship between PS height, detection date, and temporal coherence. Several key patterns emerge:

A notable inverse relationship exists between PS height and coherence values, particularly pronounced for points detected above 100m. PS points under 50m consistently show higher coherence values (0.75-0.95), while points at greater heights exhibit more variable and generally lower coherence (0.60-0.75). The observed decrease in temporal coherence with height could be partially attributed to the absence of temperature compensation in our analysis. Thermal expansion and contraction of tall buildings can significantly affect phase stability, and incorporating temperature data in the analysis could potentially improve coherence values, particularly for structures above 100m. However, even without temperature compensation, the coherence values remain sufficient for reliable height estimation up to 150m.

The temporal coherence analysis reveals that height measurements become progressively less reliable as PS height increases, with points above 150m showing the lowest temporal coherence values. This finding has important implications for the interpretation of PS-derived height measurements for tall

structures and suggests that additional validation may be necessary for measurements exceeding this height threshold.

The period up to 2015 accounts for 64.81% of all detected PS points, showing a relatively uniform spatial pattern across the study area, particularly concentrated between 114.2°E and 114.4°E. Subsequent detection periods show evolving patterns, with 2016-2018 (19.07%), 2019-2020 (9.15%), and 2021-2023 (6.98%) reflecting changes in urban development patterns and the stability of persistent scatterers over time.

#### 4.2 Spatial Patterns of Vertical Growth

The 2023 height map of Wuhan (Figure 3) shows complex patterns of vertical urban development that reflect both growth trajectories and contemporary urban planning strategies. Our analysis demonstrates distinct spatial organizations of 50 m grids across the metropolitan area, with clear patterns of clustering and gradual transitions between different urban morphologies. The analysis shows a clear concentration of tall structures (>90m, shown in dark red) along both banks of the Yangtze River, which bisects the study area from west to east. This pattern is particularly pronounced in the Jiangnan and Wuchang districts, where clusters of high-rise structures form a distinctive urban corridor along the waterfront.

The spatial analysis shows three distinct zones of vertical development radiating outward from the Yangtze River. The first zone, directly adjacent to the river, is characterized by dense clusters of buildings exceeding 50m (orange to red points). This high-intensity development is most evident between longitudes 114.2°E and 114.3°E, where the concentration of tall structures reaches its peak. The second zone forms a transition area extending approximately 2-3 kilometers from the riverbanks, exhibiting a mix of mid-rise (9-27m, yellow points) and high-rise structures (27-50m, light purple points). This creates a gradual height gradient moving away from the river. The third zone, predominantly in the northern (above 30.7°N) and southern (below 30.4°N) portions of the study area, is characterized by lower structures (<9m, blue points), showing a clear decrease in grids heights with distance from the river.

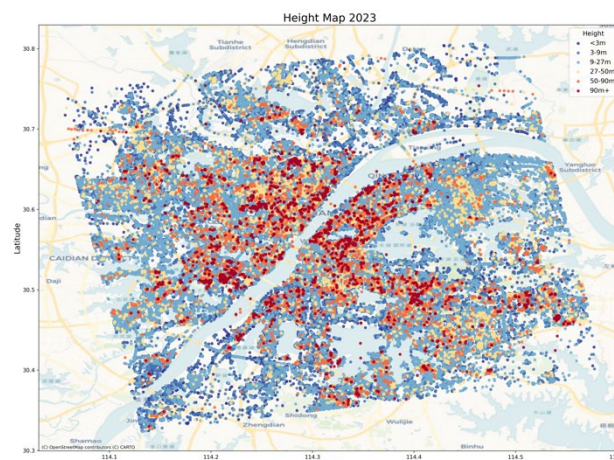


**Figure 3.** Height distribution map of Wuhan in 2023. Colors represent grids heights from <3m (dark blue) to >90m (dark red). The map shows concentrated vertical development along the Yangtze River and distinct patterns of height distribution across Wuhan.

Prominent variations in development patterns are observed between the northern and southern banks. The Hankou district,

north of the Yangtze River (around 30.6°N), displays particularly intensive vertical development with multiple distinct clusters of artificial structures exceeding 90m in height. These clusters show strong spatial correlation with the major transportation routes visible on the base map, suggesting a relationship between accessibility and vertical growth. The southern bank exhibits a more dispersed pattern of high-rise development, with smaller clusters of tall buildings distributed across a wider area. The height distribution also shows significant local variations in development intensity. Areas around major road intersections show higher concentrations of tall buildings, creating secondary nodes of vertical development away from the riverfront. This pattern is especially evident in the northeastern portion of the study area (around 114.4°E), where several distinct clusters of high-rise structures have emerged along major transportation corridors.

### 4.3 Temporal Dynamics of Construction

The temporal analysis of Wuhan's vertical growth shows distinct patterns in both construction timing and building characteristics across the study period (2015-2023). Figure 4 illustrates the spatial-temporal distribution of construction activities, showing four distinct construction periods marked by varying intensities of development and spatial preferences.

#### 4.3.1 Construction Period Analysis

The pre-2015 period accounts for the majority of detected PS points (64.81%, blue points), showing a relatively uniform distribution across the study area, particularly concentrated between 114.2°E and 114.4°E. These points likely correspond to established urban structures and historical development patterns.

Subsequent development phases show evolving patterns. The 2016-2018 period (green points, 19.07%) reflects more targeted development, with new construction concentrated along major transportation corridors and established urban nodes. Development during 2019-2020 (yellow points, 9.15%) shows further spatial concentration, especially in the northern regions near 30.7°N. The most recent phase (2021-2023, purple points, 6.98%) shows a shift toward infill development, with new construction primarily occurring within existing urban areas, suggesting a strategic focus on urban densification.

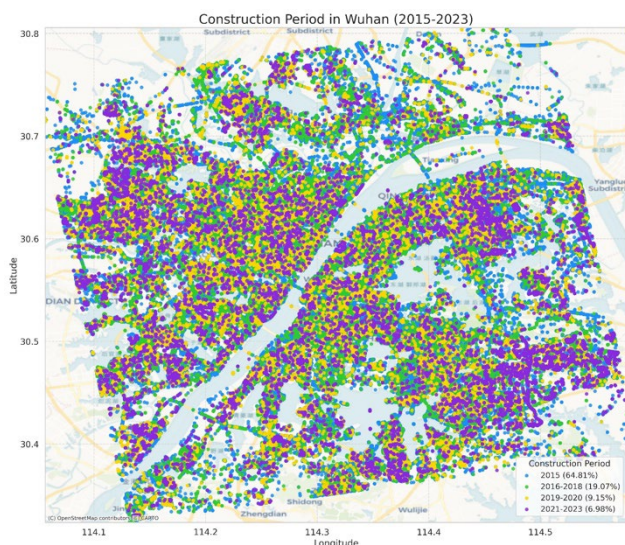


**Figure 4.** Construction Period in Wuhan (2015–2023). Colors indicate different construction periods: blue (2015), green (2016-2018), yellow (2019-2020), and purple (2021-2023).

### 4.4 District-Level Analysis

The district-level analysis shows significant spatial heterogeneity in vertical development across Wuhan's urban districts, as evidenced by both the statistical summary (Table 1) and the height distribution patterns (Figure 5).

Statistical analysis of building heights across districts shows marked variations in both the scale and character of vertical development. Jiangnan district emerges as the most vertically developed area, with the highest mean building height (29.4 meters) and a substantial standard deviation (29.18 meters), indicating significant vertical diversity in its urban fabric. This is followed by Wuchang (mean: 25.07 meters) and Jiang'an (mean: 24.1 meters), forming a trio of districts with pronounced vertical development. The building count data shows that Hongshan contains the largest number of structures (13,020), though with a more moderate mean height (20.59 meters), suggesting a different development pattern characterized by greater horizontal extent.

Table 1: District-Level Building Statistics in Wuhan

District	Count	Mean	Max
Caidian	6928	18.07	132.82
Dongxihu	7065	18.91	145.24
Hanyang	6329	23.37	194
Hongshan	13020	20.59	192.24
Jiang'an	4067	24.1	182.17
Jiangnan	3071	29.4	173.17
Jiangxia	7863	18.98	194.92
Qiaokou	3374	20.77	161.83
Qingshan	4583	19.65	175.74
Wuchang	6459	25.07	181.65

The maximum height analysis shows an interesting pattern: while Jiangnan leads in mean height, the tallest individual structures are found in Jiangxia (194.92 meters) and Hanyang (194 meters). This suggests that extreme vertical development is not necessarily correlated with overall district height characteristics. The peripheral districts of Dongxihu (mean: 18.91 meters), Caidian (18.07 meters), and Jiangxia (18.98 meters) show remarkably similar mean heights, indicating possibly coordinated development policies in these outer areas.

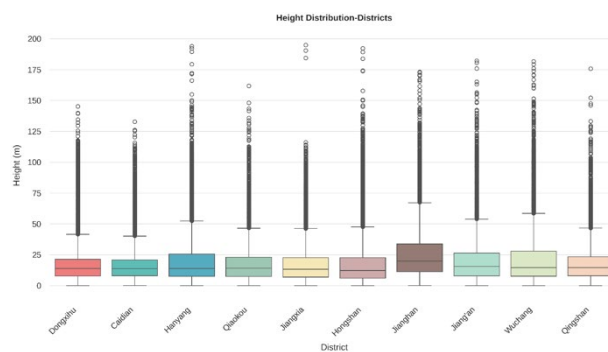


**Figure 5.** Building Height Distribution by District in Wuhan. The box plot visualization provides additional insights into the height distribution patterns:

**Quartile Distribution:** Jiangnan shows the highest median height and largest interquartile range (IQR), indicating both taller typical buildings and greater height variability. The box portion (25th to 75th percentile) extends notably higher than other districts, suggesting a systematic difference in building height policy or development pattern.

**Outlier Patterns:** All districts exhibit significant outliers above the upper whisker, but their frequency and magnitude vary considerably. Jiangnan, Hongshan, and Hanyang show particularly dense clusters of outliers above 100 meters, indicating concentrated high-rise development. In contrast, Dongxihu and Caidian show more sparse outlier patterns, suggesting more isolated instances of tall buildings.

**Height Consistency:** The lower quartile (25th percentile) remains relatively consistent across all districts (approximately 5-10 meters), while the upper quartile shows much greater variation. This suggests that while baseline development remains similar across the city, the districts differ primarily in their approach to taller structures.

**Distribution Symmetry:** Most districts show positively skewed distributions, with the box plots compressed toward the lower heights and extended whiskers and outliers toward greater heights. This asymmetry is most pronounced in peripheral districts like Dongxihu and Qingshan, where high-rise development appears more exceptional.

A comparative analysis of building counts and height distributions shows three distinct district typologies:

**High-Intensity Vertical Districts (Jiangnan, Wuchang):** Characterized by high mean heights, large standard deviations, and significant numbers of outlier tall buildings.

**Mixed-Development Districts (Jiang'an, Hanyang):** Showing moderate mean heights but substantial maximum heights, indicating selective high-rise development.

**Horizontal Expansion Districts (Dongxihu, Caidian, Jiangxia):** Exhibiting lower mean heights but large building counts, suggesting prioritization of horizontal over vertical development.

The temporal pattern of height development varies significantly among districts. Wuchang and Jiangnan showed accelerated vertical growth in recent years (2022-2023), while Jiang'an maintained steady growth throughout the study period. The contrasting trends in Qiaokou and Hanyang, where periods of decline were observed, suggest that vertical development patterns are influenced by district-specific factors rather than following a uniform citywide trend.

These findings highlight the complex relationship between district-level planning policies, development opportunities, and local constraints in shaping Wuhan's vertical urban landscape. The clear statistical differences between districts suggest that vertical development is not merely a function of proximity to the city center but reflects more complex patterns of urban evolution and planning strategies.

## 5. Limitations

Despite the Stack On-off model's effectiveness in monitoring vertical urban growth, several limitations specific to Sentinel-1 data implementation warrant consideration. The primary constraint lies in the methodology's requirement for a substantial recent stack of 25-30 images for reliable processing, which introduces an inherent temporal lag in detecting the most recent urban changes. While Sentinel-1's consistent 12-day temporal sampling provides regular data acquisition, its relatively lower spatial resolution compared to X-band sensors can limit the detection of fine-scale urban changes, particularly in areas with

dense urban development. Additionally, the coherence analysis revealed challenges in maintaining high measurement reliability for structures exceeding 100 meters in height, as evidenced by the decreasing coherence values for the higher PS points. This height-dependent limitation affects the accuracy of measurements for very tall structures, suggesting the need for additional validation measures when monitoring high-rise developments. The methodology's reliance on amplitude stability for point selection may also result in missing temporary construction phases or rapid changes that don't persist long enough to be captured within the recent stack window, particularly in areas undergoing intensive development.

## 6. Discussion and Conclusion

This study presents a novel adaptation of PSInSAR methodology for monitoring vertical urban growth, demonstrating its effectiveness through a comprehensive analysis of Wuhan's urban development from 2015 to 2024. The proposed Stack On-Off model approach offers several significant advantages over traditional PSInSAR processing while providing valuable insights into the patterns and dynamics of urban vertical expansion. The streamlined PSInSAR Stack On-Off approach introduces important methodological improvements in urban monitoring. By focusing initial PS point extraction on recent imagery (2023-2024) before analyzing the full temporal stack, the method significantly reduces computational requirements while maintaining monitoring capability. In our experimental testing, this approach completed the analysis in approximately 2 days compared to a week required by the traditional PSInSAR on-off method, using the same hardware configuration (Intel Core i5, 16GB RAM). This substantial reduction in processing time is achieved through reduced initial data volume for PS detection (30 images versus 212), focused processing of pre-selected PS points for the full temporal analysis, and optimized sequential processing workflow. This efficiency gain, coupled with the robust dual-threshold strategy for PS point selection, makes the approach particularly suitable for long-term, large-scale monitoring of urban vertical growth.

The method's ability to detect both construction events ( $T_{ON}$ ) and potential demolitions ( $T_{OFF}$ ) provides a comprehensive view of urban dynamics that goes beyond simple height measurements. The implementation of sophisticated coherence analysis and spatial clustering techniques (DBSCAN) further enhances the reliability of height estimations and helps identify meaningful patterns in urban development.

The analysis shows distinct patterns in Wuhan's vertical urban growth that reflect both planned development strategies and organic urban evolution. The spatial distribution of building heights shows a correlation with proximity to the Yangtze River, with the highest concentration of tall structures along the riverfront, particularly in the Jiangnan and Wuchang districts. This pattern suggests that waterfront areas continue to be prime locations for intensive vertical development, likely due to their strategic importance and high land values. The temporal analysis indicates a shift in development patterns over the study period. While pre-2015 development (64.81% of structures) showed relatively uniform spatial distribution, subsequent periods exhibit increasingly targeted development strategies. The decline in new construction rates from 2015 to 2023, stabilizing at 25,000-30,000 buildings annually, suggests a maturing urban development cycle with a greater emphasis on strategic intensification rather than extensive expansion.

The significant variations in vertical development across districts highlight the complexity of urban growth patterns. The emergence of Jiangnan as the most vertically developed district (mean height 29.4m) contrasts with the more horizontally oriented growth in peripheral districts like Dongxihu and Caidian (mean heights ~18m). This disparity reflects both the historical evolution of these districts and their current development priorities. The identification of three distinct district typologies - High-Intensity Vertical, Mixed-Development, and Horizontal Expansion - provides a useful framework for understanding Wuhan's urban development strategy. This pattern suggests a deliberate policy of concentrated vertical growth in central districts while maintaining more moderate development intensities in peripheral areas.

The findings have several important implications for urban planning and policy. The concentration of vertical development along transportation corridors and waterfront areas suggests the need for continued infrastructure investment in these high-density zones. The varying patterns of district-level development indicate successful implementation of differentiated planning strategies, though they may require periodic reassessment to ensure alignment with changing urban needs. The observed stabilization in construction rates points to a potential maturation of Wuhan's urban development cycle, suggesting future planning may need to focus more on renewal and optimization rather than expansion.

While this study demonstrates the effectiveness of the Stack On-Off approach, several areas need further investigation. Integration with other data sources, such as optical imagery and social-economic data, could provide deeper insights into the drivers of vertical urban growth. Extension of the methodology to other rapidly developing cities could help validate its broader applicability and identify common patterns in urban vertical growth. Development of automated methods for identifying and classifying different types of vertical growth patterns could enhance the utility of this approach for urban planners.

This study demonstrates that the PSInSAR Stack On-Off model provides an effective and efficient method for monitoring vertical urban growth, offering valuable insights into the complex dynamics of urban development. The analysis of Wuhan's vertical growth patterns shows a city in transition, with clear spatial preferences for vertical development and distinct district-level strategies for urban intensification. These findings not only contribute to our understanding of urban vertical growth patterns but also provide practical insights for urban planning and policy development in rapidly growing metropolitan areas. The success of this methodology in capturing both spatial and temporal aspects of urban vertical growth suggest its potential applicability to other rapidly developing cities, particularly where traditional monitoring methods may be impractical or cost-prohibitive. As cities worldwide continue to grow vertically in response to land scarcity and population pressure, the ability to efficiently monitor and understand these changes becomes increasingly crucial for informed urban planning and management.

## References:

Afzal, Z., Balz, T., Ali, M., Asghar, A., Hussain, S., Sunantha, O., 2023. Geological Interpretation of the Deformation Obtained by PSInSAR in Islamabad and Rawalpindi. *Int. Arch. Photogramm. Remote Sens. Spatial Inf. Sci.*, XLIV-3/W2-2023, 33-40.

China Statistics Press, 2020. *China City Statistical Yearbook-2020*. China Statistics Press, Beijing.

Crosetto, M., Monserrat, O., Cuevas-González, M., Devanthery, N., Crippa, B., 2016. Persistent Scatterer Interferometry: A Review. *ISPRS J. Photogramm. Remote Sens.*, 115, 78-89.

Ferretti, A., Prati, C., Rocca, F., 2001. Permanent Scatterers in SAR Interferometry. *IEEE Trans. Geosci. Remote Sens.*, 39(1), 8-20.

Letsios, V., Faraslis, I., Stathakis, D., 2023. Monitoring Building Activity by Persistent Scatterer Interferometry. *Remote Sens.*, 15(4), 950.

Li, X., Zhou, Y., Zhao, M., Zhao, X., 2020a. Harmonization of DMSP and VIIRS Nighttime Light Data from 1992-2021 at the Global Scale. *Sci. Data*, 7, 168.

Li, X., Zhou, Y., Gong, P., Seto, K.C., Clinton, N., 2020b. Developing a Method to Estimate Building Height from Sentinel-1 Data. *Remote Sens. Environ.*, 240, 111705.

Liu, K., Ma, H., Cai, Z., Zhang, L., 2020. Building Extraction from Airborne LiDAR Data. *Remote Sens.*, 12(17), 2849.

Perissin, D., 2017. Geometric Processing: Active Sensor Modeling and Calibration (SAR). In: *Comprehensive Remote Sensing*. Elsevier, Oxford, pp. 171-193.

Prakash, A., Diksha, Kumar, A., 2023. Measuring Vertical Urban Growth of Patna Urban Agglomeration Using Persistent Scatterer Interferometry SAR (PSInSAR) Remote Sensing. *Remote Sens.*, 15(14), 3687.

Sun, Z., Kang, D., Jiao, H., Yang, Y., Xue, W., Wu, H., Liu, L., Su, Y., Peng, Z., 2023. Spatial and Temporal Evolution of the Characteristics of Spatially Aggregated Elements in an Urban Area: A Case Study of Wuhan, China. *ISPRS Int. J. Geo-Information*, 12(11), 448.

Torres, R., Snoeij, P., Geudtner, D., Bibby, D., Davidson, M., Attema, E., Potin, P., Rommen, B.Ö., Floury, N., Brown, M., 2012. GMES Sentinel-1 Mission. *Remote Sens. Environ.*, 120, 9-24.

UN Desa, 2019. *World Population Prospects 2019: Highlights (ST/ESA/SER.A/423)*. United Nations, Department of Economic and Social Affairs, Population Division, New York.

United Nations, 2018. *World Urbanization Prospects 2018*. UN Department of Economic and Social Affairs, New York.

Wang, H., Liu, Y., Zhang, B., Xu, S., Jia, K., Hong, S., 2018. Analysis of Driving Forces of Urban Land Expansion in Wuhan Metropolitan Area Based on Logistic-GTWR Model. *Trans. Chinese Soc. Agric. Eng.*, 34(19), 255-265.

Wang, L., Li, Z., Zhang, Z., 2022. City Profile: Wuhan 2004-2020. *Cities*, 122, 103585.

Wuhan Municipal Statistics Bureau, 2020. *Wuhan Statistical Yearbook 2020*. China Statistics Press, Wuhan.

Yague-Martinez, N., Prats-Iraola, P., Gonzalez, F.R., Brcic, R., Shau, R., Geudtner, D., Eineder, M., Bamler, R., 2016.

Interferometric Processing of Sentinel-1 TOPS Data. IEEE  
Trans. Geosci. Remote Sens., 54(4), 2220-2234.

Zhang, Q., Seto, K.C., 2011. Mapping Urbanization Dynamics at  
Regional and Global Scales Using Multi-Temporal DMSP/OLS  
Nighttime Light Data. Remote Sens. Environ., 115(9), 2320-  
2329.